Supporting information

Naphthalene as building block for organic laser dyes with smaller energy gaps and enhanced stability

Yuya Oyama,[a,b] Masashi Mamada,[a,b,c*] Akihiro Kondo,[d*] Chihaya Adachi[a,b,c,e,*]

[a] *Center for Organic Photonics and Electronics Research (OPERA), Kyushu University, Fukuoka 819-0395, Japan*

[b] *JST, ERATO, Adachi Molecular Exciton Engineering Project c/o Center for Organic Photonics and Electronics Research (OPERA), Kyushu University, Nishi, Fukuoka 819-0395, Japan*

[c] *Academia-Industry Molecular Systems for Devices Research and Education Center (AIMS), Kyushu University, Nishi, Fukuoka 819-0395, Japan*

[d] *R &D Center, NIPPON SHIZAI CO., LTD. 923-2, Touendo, Aisho-cho, Echi-gun, Shiga, 529-1325, Japan*

[e] *International Institute for Carbon Neutral Energy Research (WPI-I2CNER), Kyushu University, Nishi, Fukuoka 819-0395, Japan*

*Corresponding author.

E-mail address: mamada@opera.kyushu-u.ac.jp (M. Mamada)

E-mail address: a-kondo@nippon-shizai.com (A. Kondo)

E-mail address: adachi@cstf.kyushu-u.ac.jp (C. Adachi)

Contents:

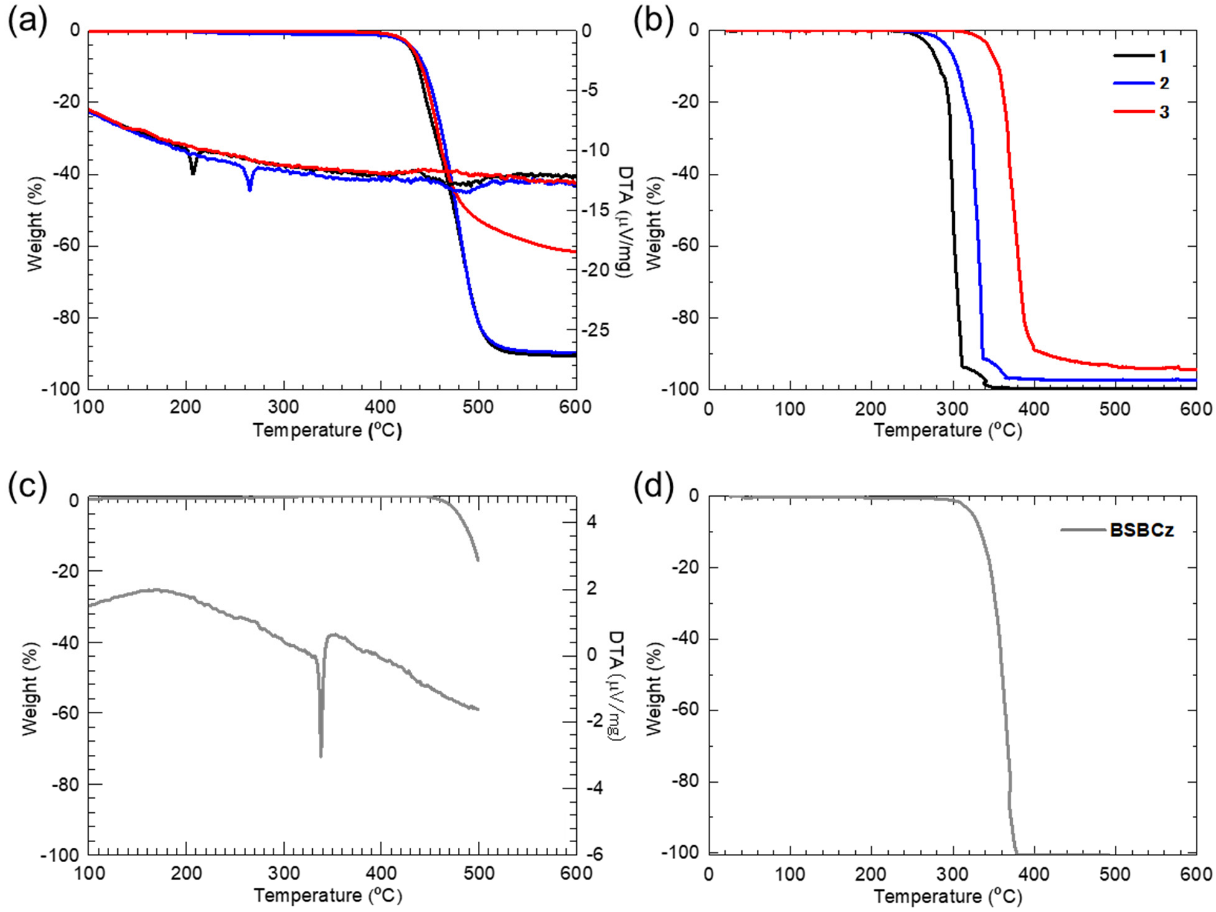

Fig. S1. TG-DTA for **1**–**3** and BSBCz. (a) TG-DTA at 10^5 Pa and (b) TG at 1 Pa for **1**, **2** and **3**. (c) TG-DTA at 10^5 Pa and (d) TG at 1 Pa for BSBCz. (5 wt% loss temperature represents the decomposition at ambient pressure and sublimation in vacuum.)

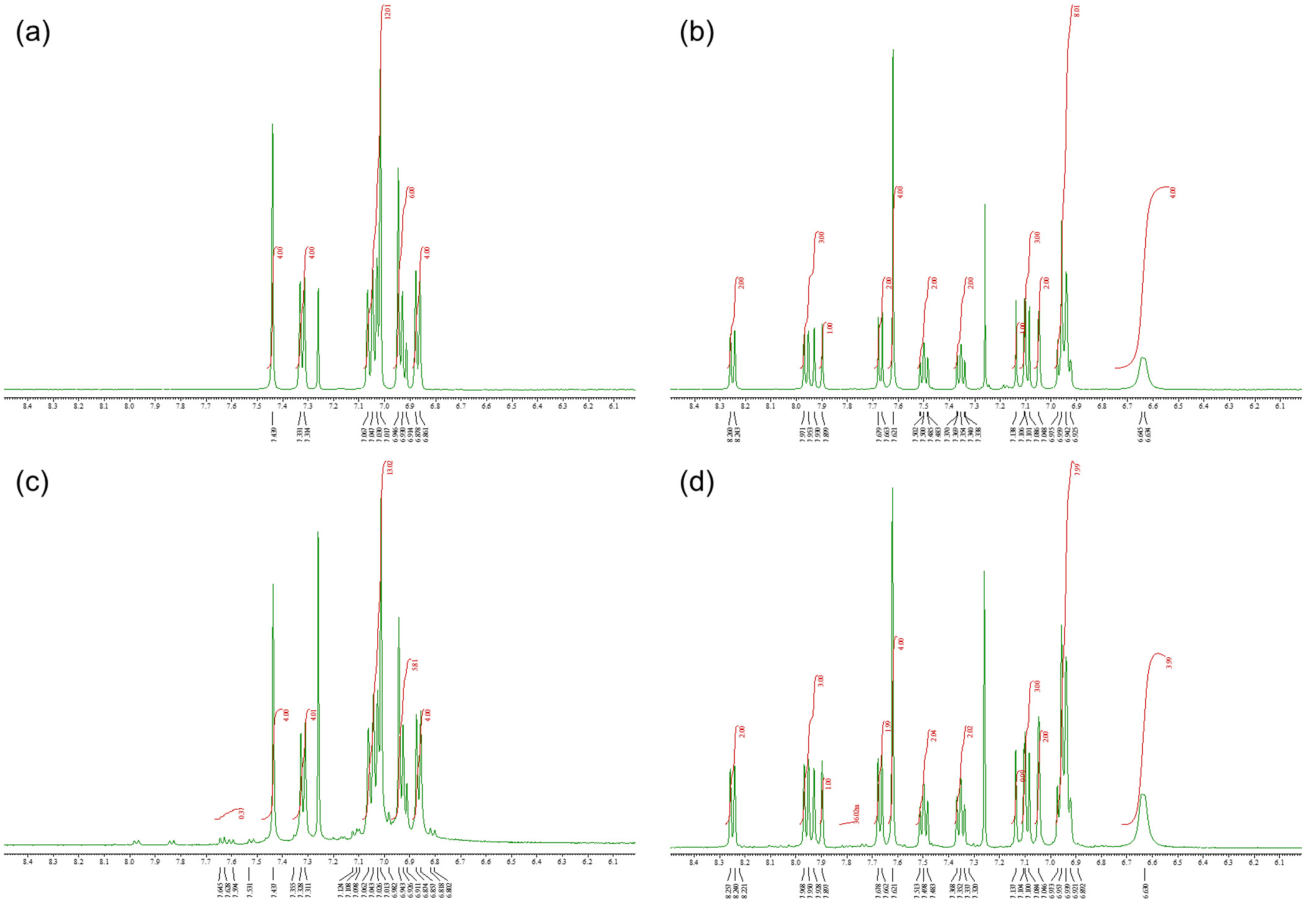

Fig. S2. ^{1}H NMR spectra before and after heating. ^{1}H NMR spectra of (a) **1** before, (b) **2** before, (c) **1** after, and (d) **2** after heating at 300 °C.

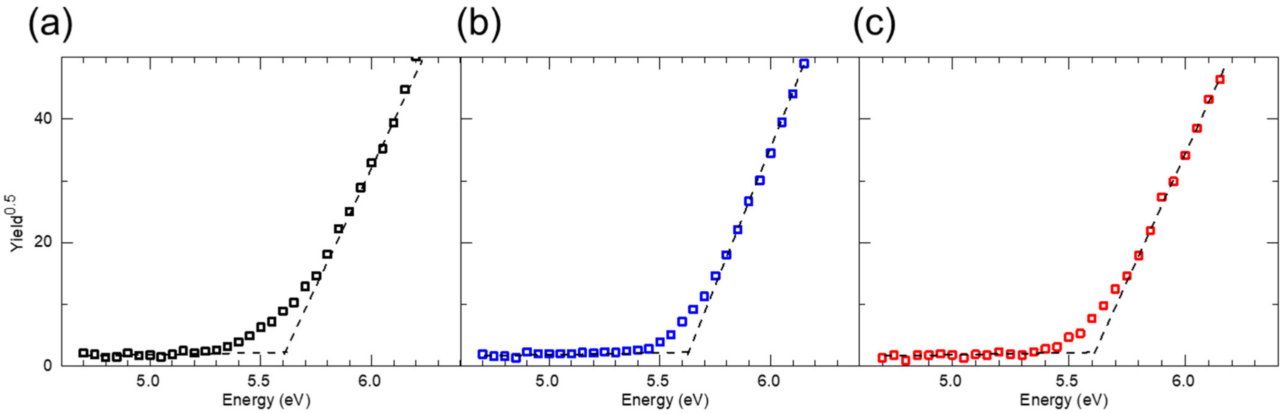

Fig. S3. Photoelectron yield spectroscopy measurements for neat films of (a) **1**, (b) **2** and (c) **3** recorded with a Riken Keiki AC-3.

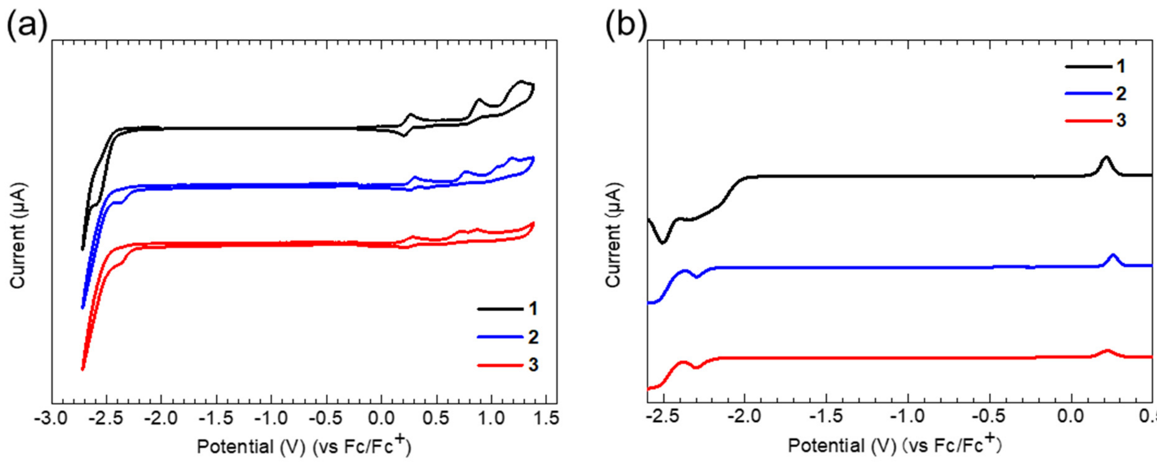

Fig. S4. Cyclic voltammograms (CV) and differential pulse voltamograms (DPV). (a) CV and (b) DPV of **1**, **2** and **3** in dichloromethane (vs Fc/Fc$^+$).

Table S1. Redox potentials, HOMO-LUMO levels and energy gaps of **1**, **2** and **3**.

Compd.	CV		DPV		HOMO (eV)	LUMO (eV)	E_g^{redox} (V)	E_g^{opt} (V)
	E_{ox} (V)	E_{red} (V)	E_{ox} (V)	E_{red} (V)				
1	0.240	−2.55	0.217	−2.49	−5.02	−2.32	2.70	2.70
2	0.285	−2.37	0.256	−2.30	−5.06	−2.50	2.56	2.48
3	0.255	−2.37	0.222	−2.30	−5.01	−2.50	2.51	2.39

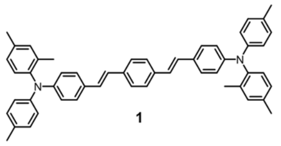 1	top view	front view
LUMO	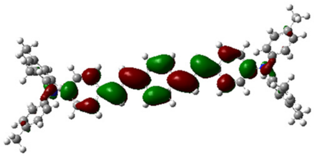	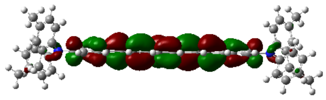
HOMO	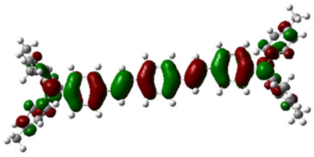	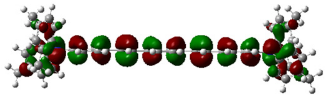
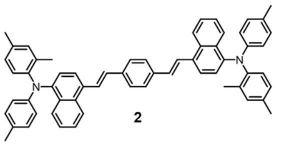 2	top view	front view
LUMO	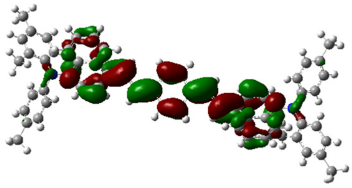	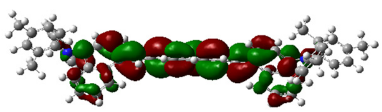
HOMO	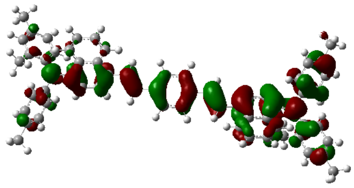	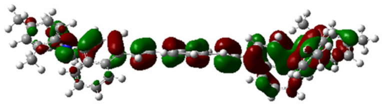
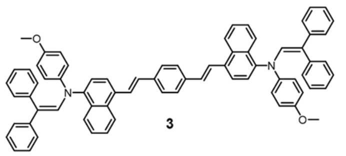 3	top view	front view
LUMO	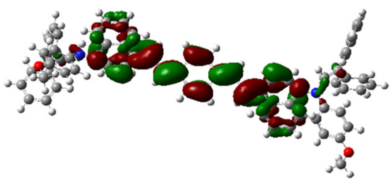	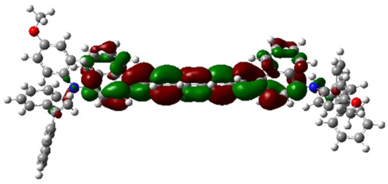
HOMO	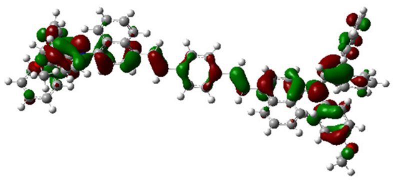	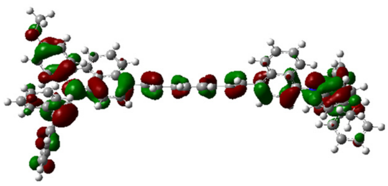

Fig. S5. Molecular orbitals of **1**, **2** and **3**.

Table S2. Calculated energies and first vertical excitation energies (VEE) of **1**, **2** and **3**.

Compd.	HOMO [eV]	LUMO [eV]	Gap [eV]	S_1-vertical [eV]	VEE
1	−4.76	−1.89	2.87	−57688.636	2.5546 eV, 485 nm, *f* = 2.4058
2	−4.89	−2.10	2.79	−66050.371	2.4243 eV, 511 nm, *f* = 1.6406
3	−4.90	−2.26	2.64	−82651.737	2.2708 eV, 546 nm, *f* = 1.2741

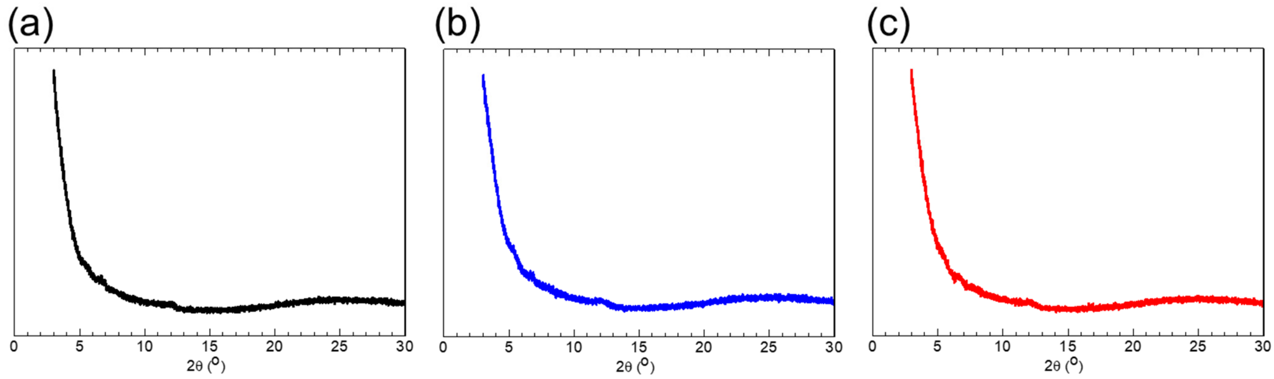

Fig. S6. Out-of-plane X-ray diffractograms of (a) **1**, (b) **2** and (c) **3** in neat films.

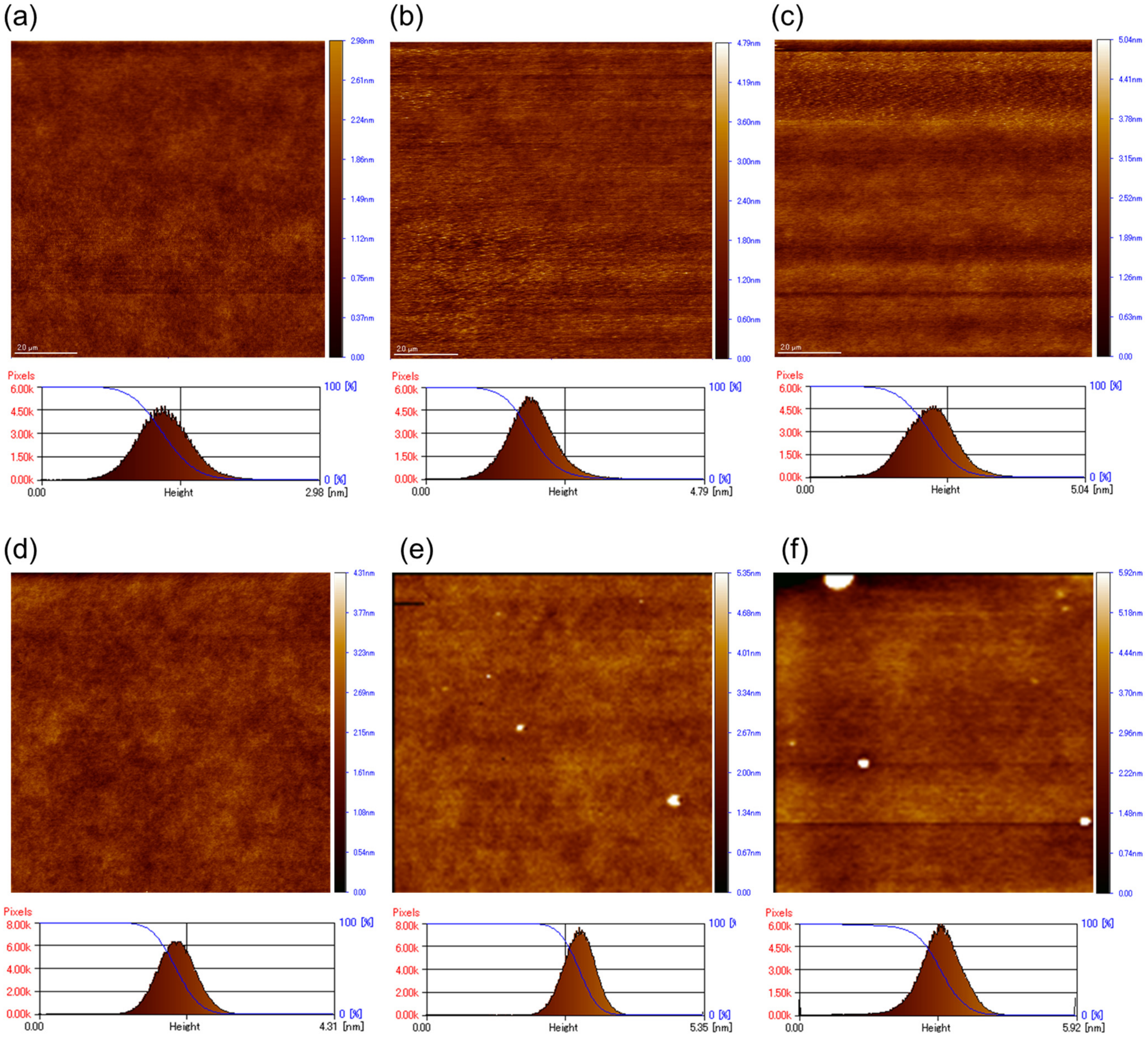

Fig. S7. AFM images for doped and neat films. (a) **1**-doped CBP, (b) **2**-doped CBP, (c) **3**-doped CBP, (d) **1**-neat, (e) **2**-neat and (f) **3**-neat films. The room mean square (RMS) roughness were 0.23, 0.33 and 0.37 for **1**-doped, **2**-doped and **3**-doped films, respectively, and 0.22, 0.25 and 0.46 nm for **1**-neat, **2**-neat and **3**-neat films, respectively. Note that the RMS for **3**-neat film without a granular lump was 0.29 nm.

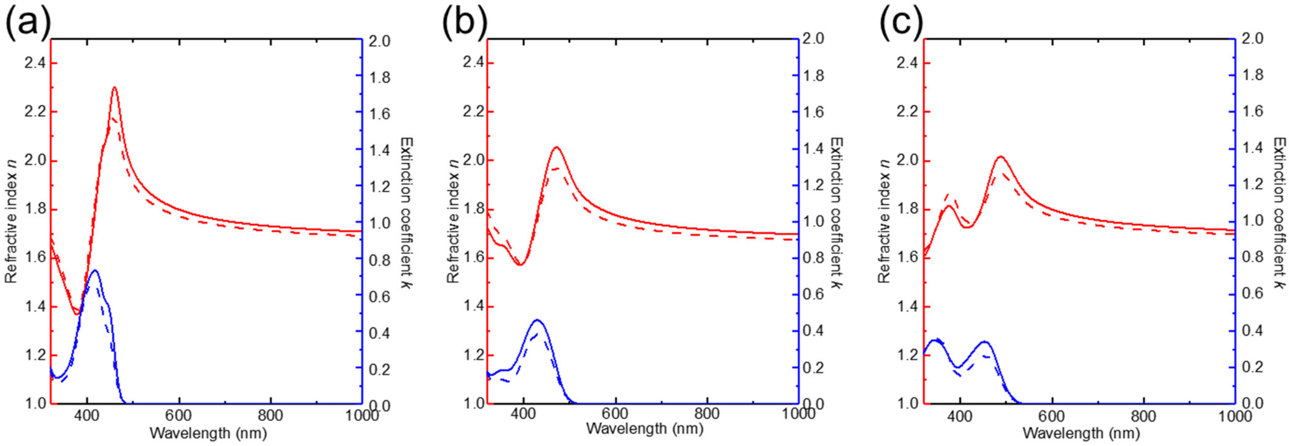

Fig. S8. Variable-angle spectroscopic ellipsometry measurements of (a) **1**, (b) **2** and (c) **3** in neat films (solid lines: ordinary, and dashed lines: extraordinary).

Table S3. Ordinary and extraordinary refractive indices and horizontally orientation order parameters of **1**, **2** and **3** in neat films.

Sample	Ordinary refractive index n_o[a)]	Extraordinary refractive index n_e[a)]	Birefringence $\Delta n = n_o - n_e$	Orientation order parameter S[b)]	n_o at the ASE wavelength[c)]	n_e at the ASE wavelength[c)]
1	1.70	1.67	0.0265	–0.039	1.91	1.86
2	1.82	1.78	0.0385	–0.060	1.84	1.80
3	1.85	1.82	0.0358	–0.080	1.85	1.81

a) At 550 nm. b) $S = (3\cos^2\theta - 1)/2 = (k_e - k_o)/(k_e + 2k_o)$, where k_o and k_e are the ordinary and extraordinary extinction coefficients at the peak wavelength. c) At 518, 548 and 567 nm for **1**, **2** and **3**, respectively.

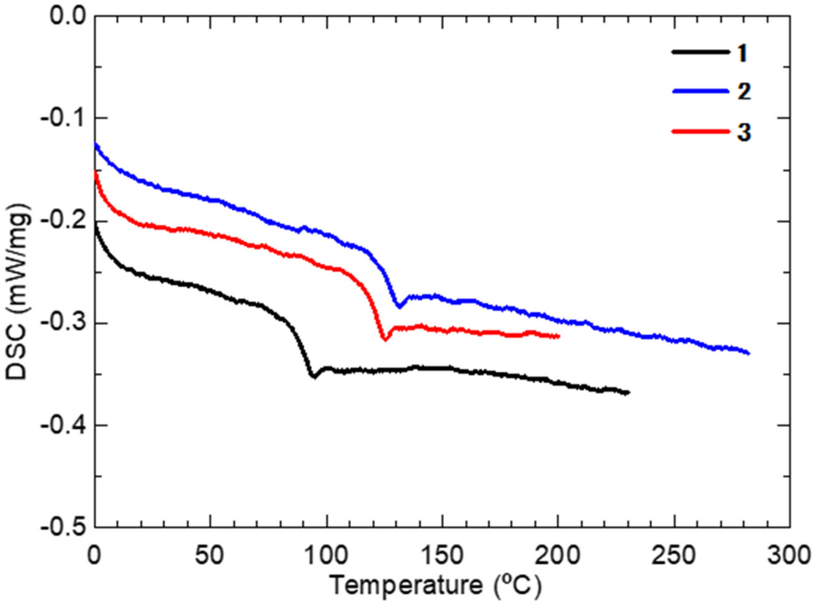

Fig. S9. DSC curves of 1, 2 and 3. The glass transition temperatures (T_g) were 90.7, 127.8 and 122.0 °C for **1**, **2** and **3**, respectively.

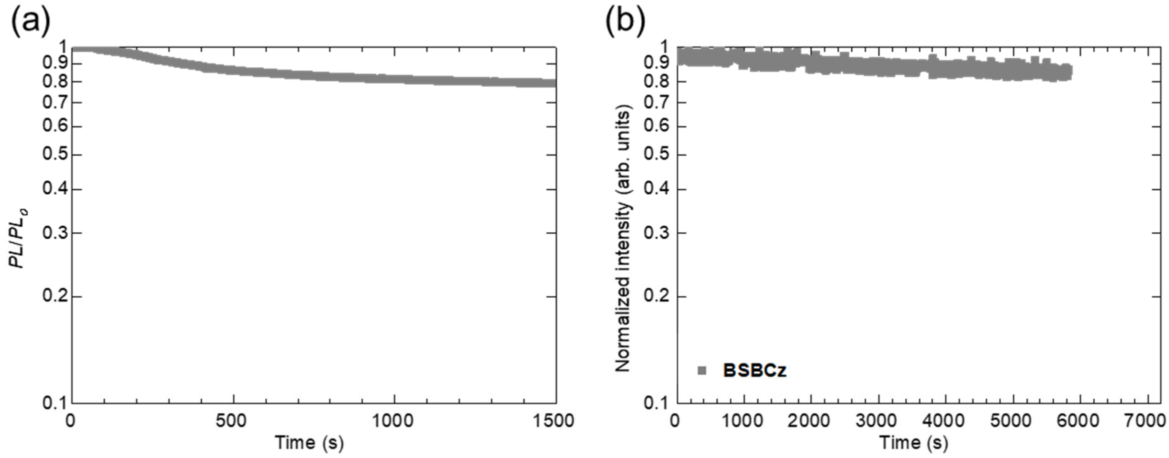

Fig. S10. Photo-stability for BSBCz. (a) PL and (b) ASE intensities normalized to the initial as a function of time for BSBCz irradiated by continuous-wave laser light at 355 nm and a nitrogen gas laser at 337 nm, respectively. Excitation intensity: (a) 120 mW cm^{-2} and (b) 280 μJ cm^{-2}.

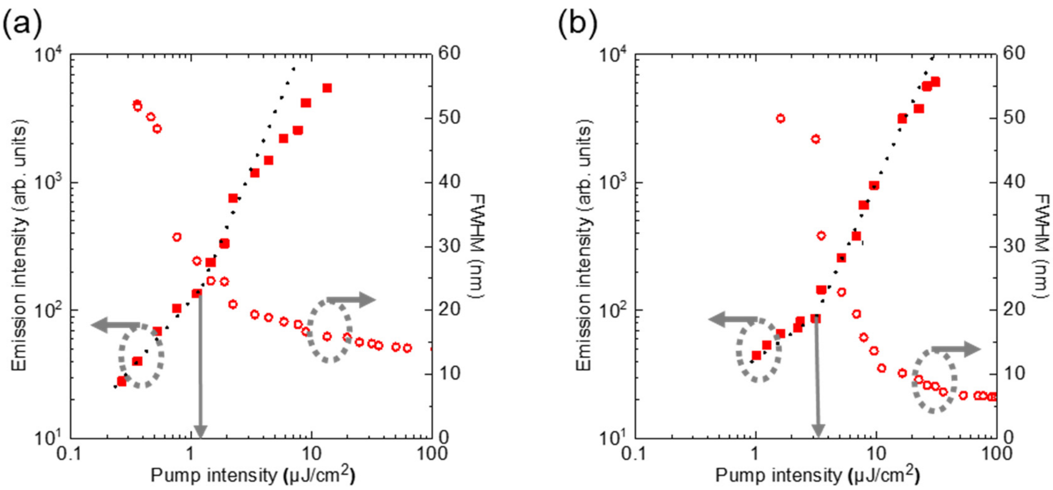

Fig. S11. ASE properties of **3** in (a) doped CBP film and (b) neat film.

Methods. S1. Calculation of the absorption and stimulated emission cross sections (σ_{abs} and σ_{em})[S1]

The absorption cross section $\sigma_{abs}(\lambda)$ was estimated by the following formula.

$$\sigma_{abs}(\lambda) = \frac{1000\varepsilon(\lambda)\ln 10}{N_A}$$

Here, $\varepsilon(\lambda)$ is the molar absorption coefficient and N_A is the Avogadro number.
Next, the stimulated emission cross section $\sigma_{em}(\lambda)$ was evaluated by the following formula.

$$\sigma_{em}(\lambda) = \frac{\lambda^4 E_f(\lambda)}{8\pi n^2(\lambda) c \tau_f}$$

$E_f(\lambda)$ corresponds to the distribution of PL efficiency and n is the dispersion of the refractive index. τ_f corresponds to the fluorescence lifetime.

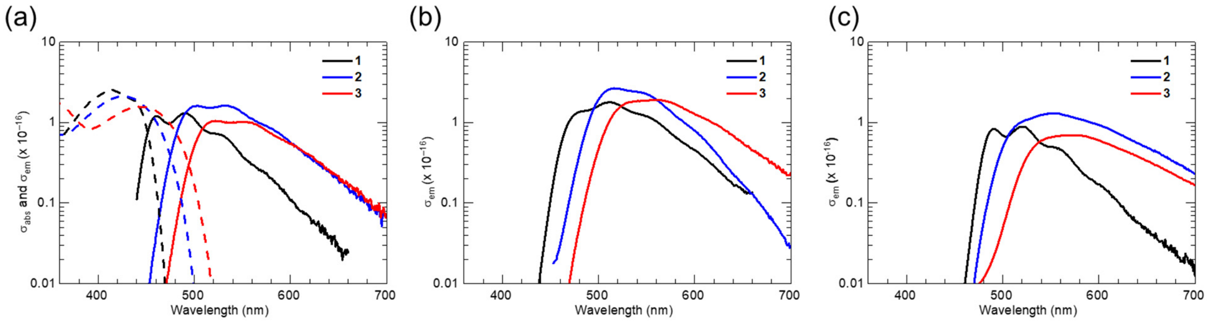

Fig. S12. Absorption and stimulated emission cross sections (σ_{abs} and σ_{em}) spectra (a) in solution, and σ_{em} (b) in doped films and (c) in neat films for **1**, **2** and **3**.

Data S1. NMR spectra of **1–3**

[1]H NMR spectrum of **1** (500 MHz, $CDCl_3$, 300K)

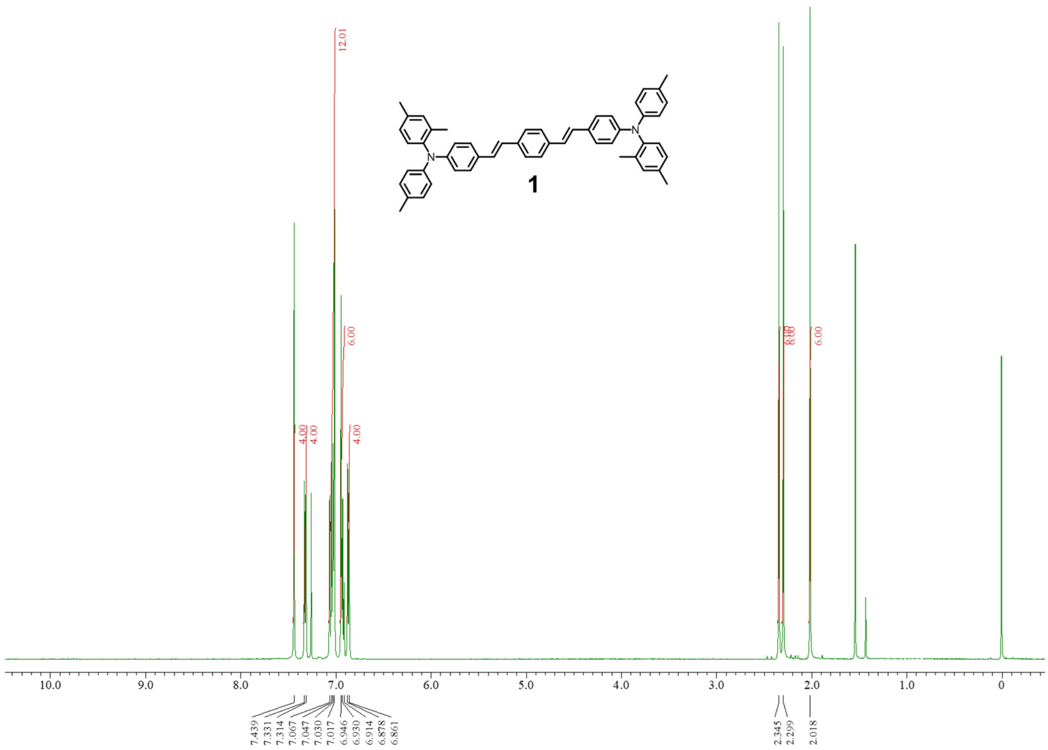

[13]C NMR spectrum of **1** (125 MHz, $CDCl_3$, 300K)

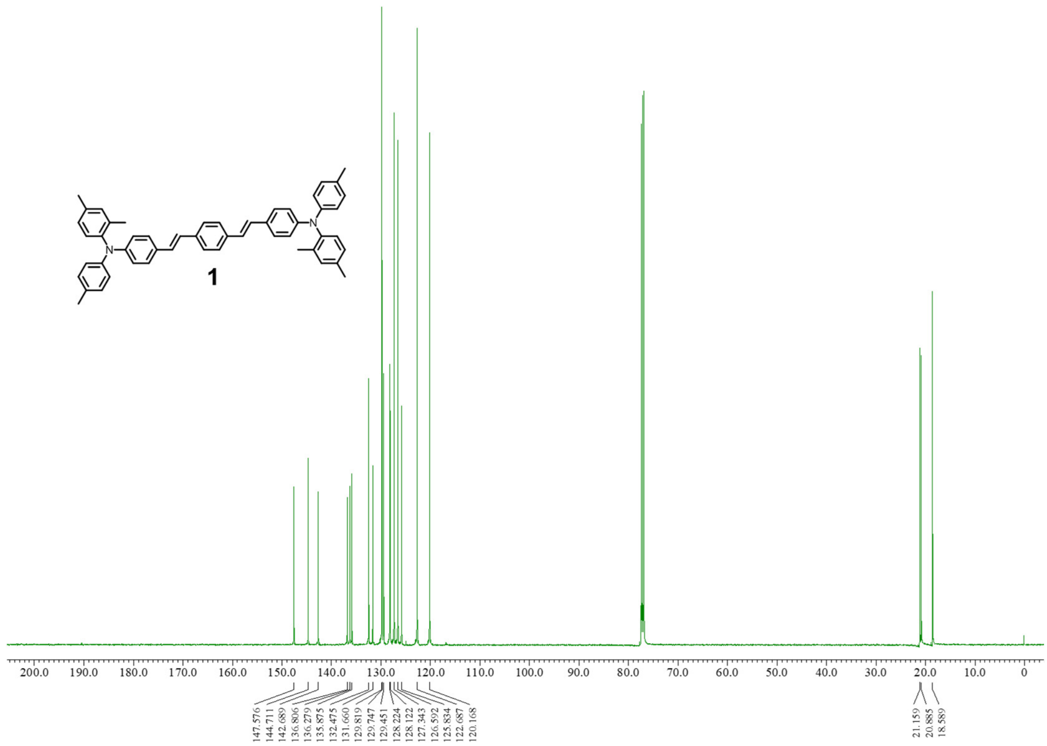

^{1}H NMR spectrum of **2** (500 MHz, $CDCl_3$, 300K)

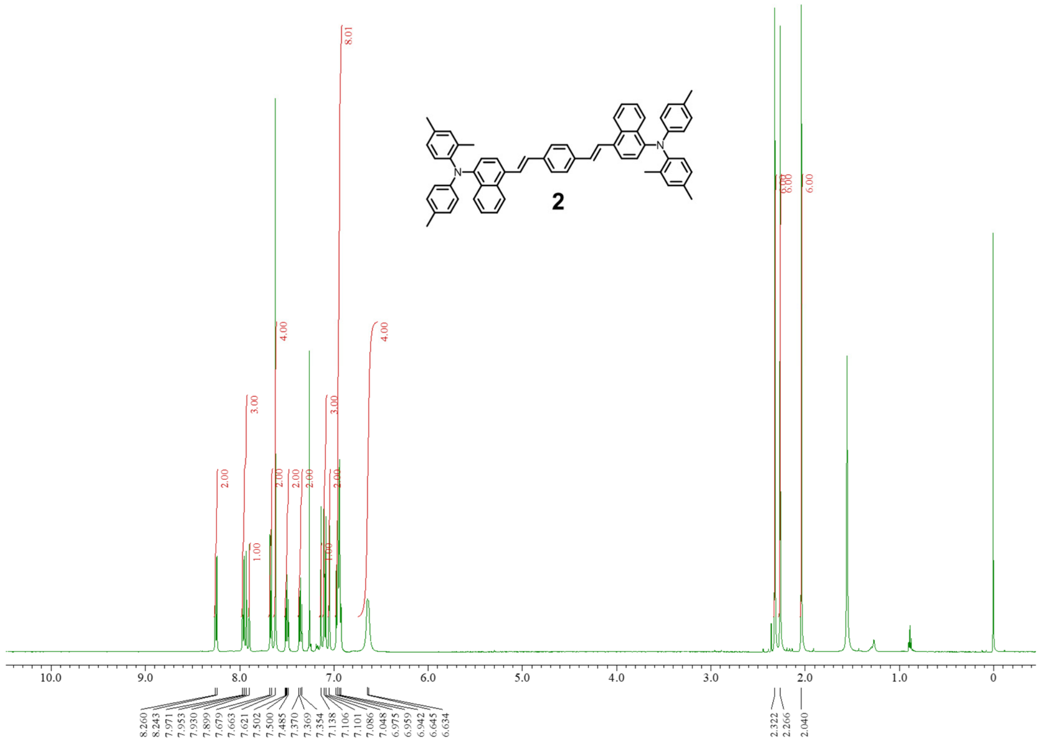

^{13}C NMR spectrum of **2** (125 MHz, $CDCl_3$, 300K)

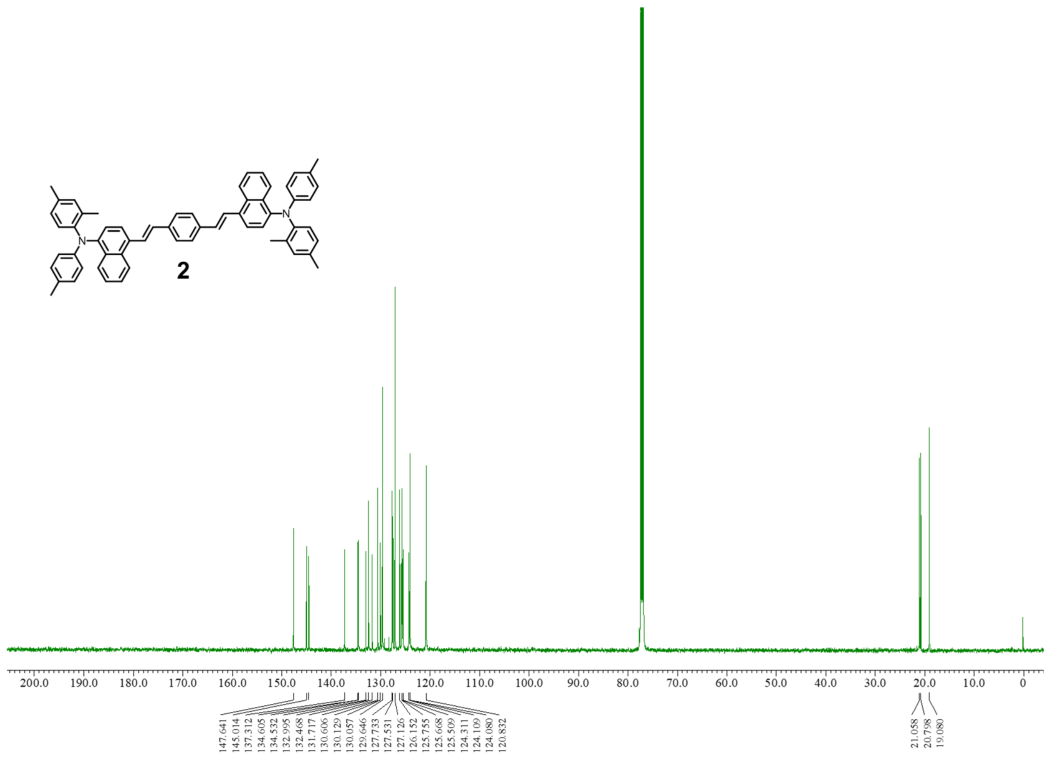

^1H NMR spectrum of **3** (500 MHz, $CDCl_3$, 300K)

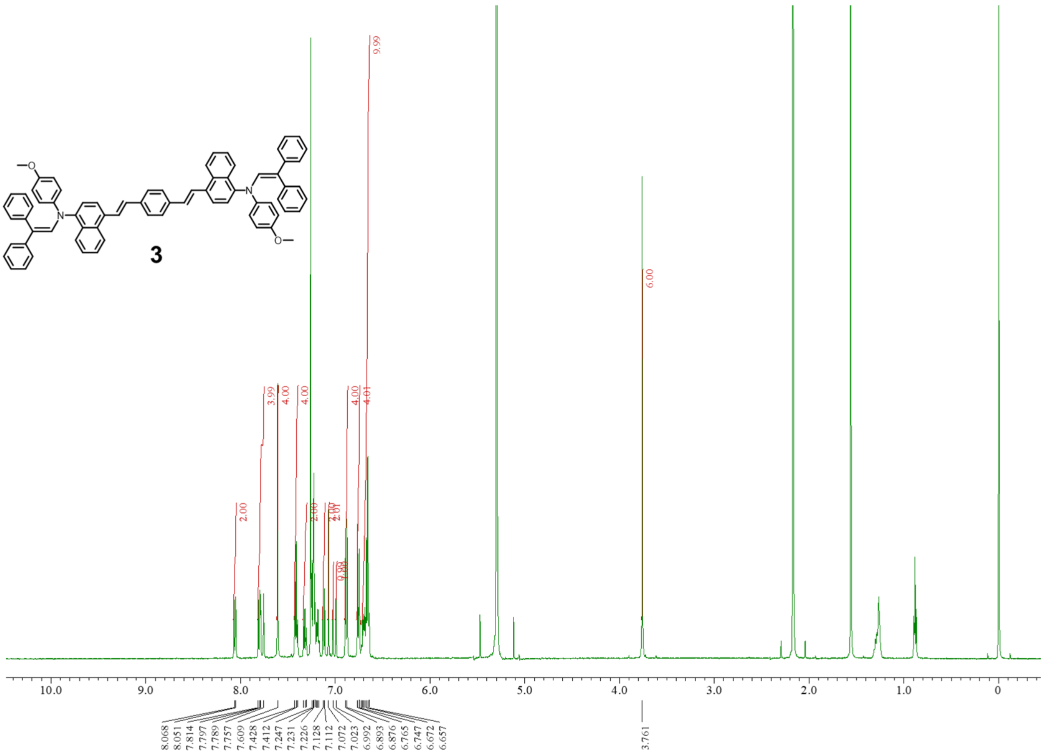

^{13}C NMR spectrum of **3** (125 MHz, $CDCl_3$, 300K)

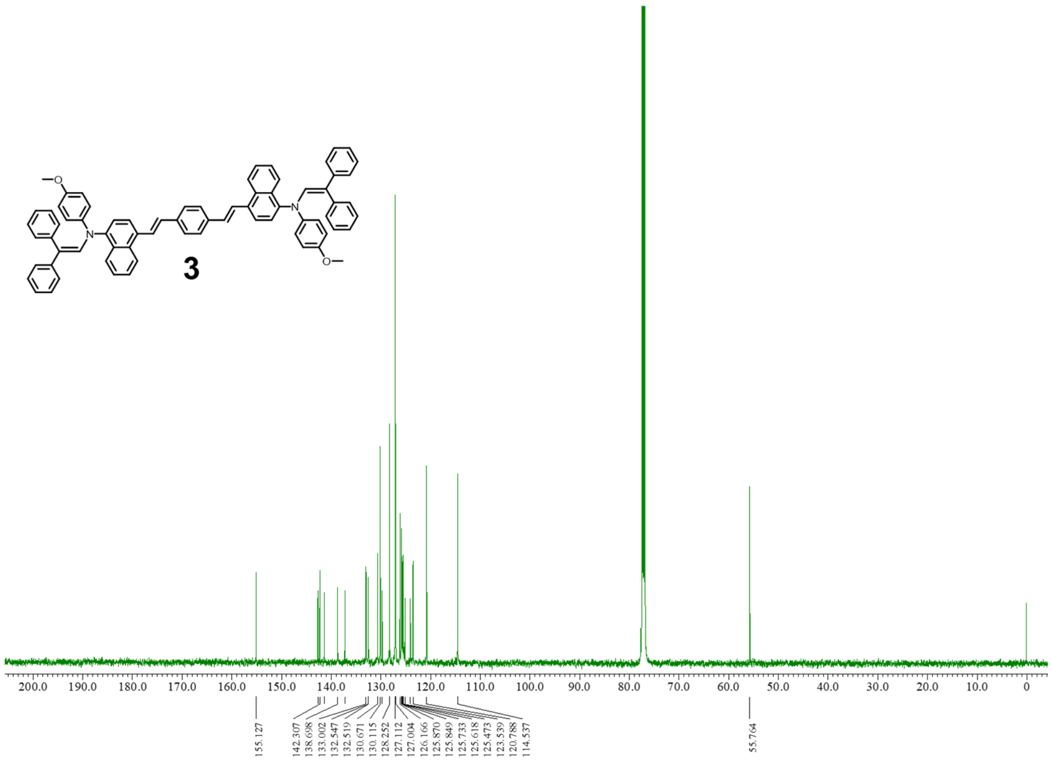

H-H COSY NMR spectrum of **1** (500 MHz, $CDCl_3$, 300K)

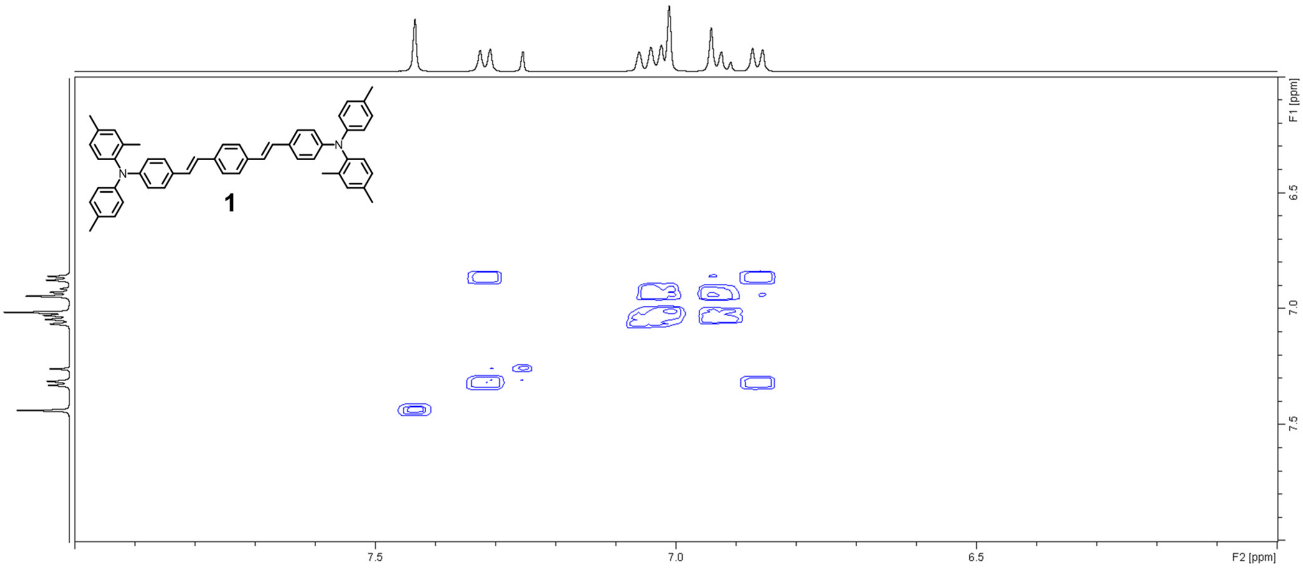

H-H COSY NMR spectrum of **2** (500 MHz, $CDCl_3$, 300K)

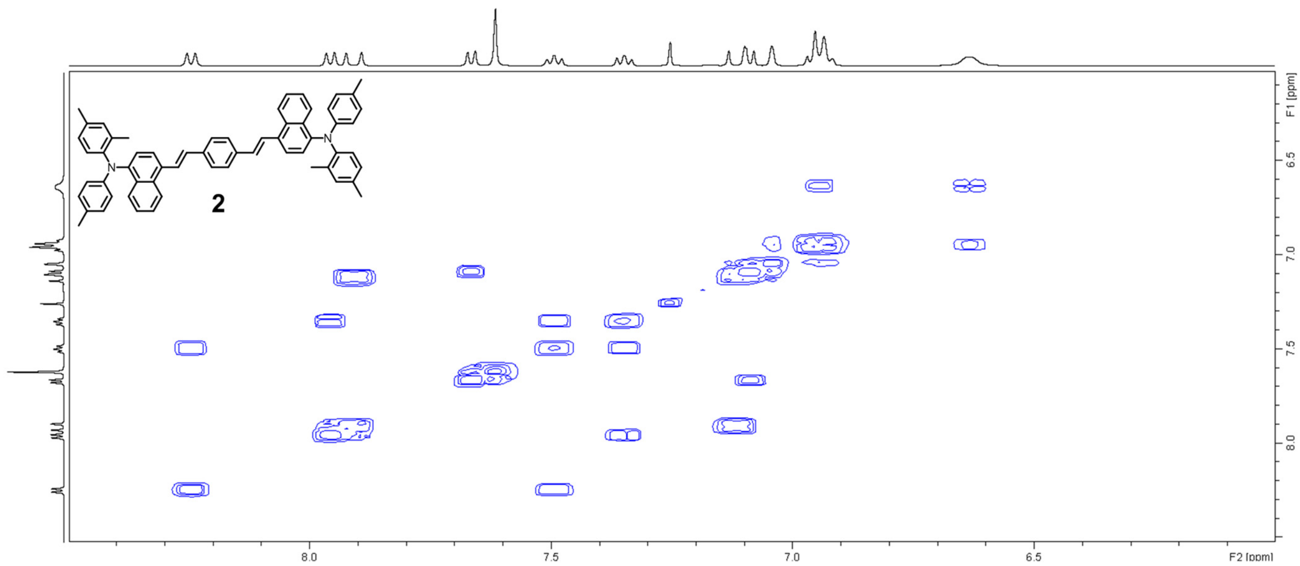

H-H COSY NMR spectrum of **3** (500 MHz, $CDCl_3$, 300K)

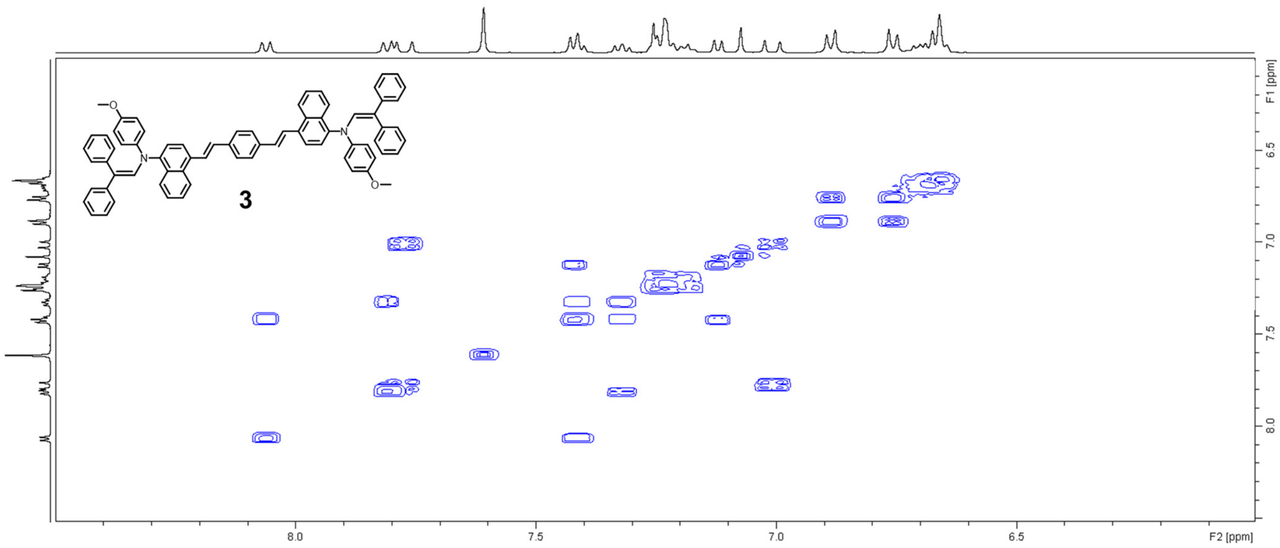

Supplementary Reference

(S1) H. Nakanotani, C. Adachi, S. Watanabe and R. Katoh, *Appl. Phys. Lett*. 2007, **90**, 231109.